chemosensors

MDPI

*Article*

# Stretching the Limits of Refractometric Sensing in Water Using Whispering-Gallery-Mode Resonators

**Kevin Soler-Carracedo [1,*], Antonia Ruiz [2,3], Susana Ríos [2], Sergio de Armas-Rillo [2], Leopoldo L. Martín [2,3], Martin Hohmann [4,5], Inocencio R. Martín [2,6] and Fernando Lahoz [2,3,*]**

1 Faculty of Chemistry, Adam Mickiewicz University, Uniwersytetu Poznańskiego 8, 61-614 Poznań, Poland
2 Departamento de Física, Universidad de La Laguna, Apdo. 456, E-38200 San Cristóbal de La Laguna, Spain; antruiz@ull.edu.es (A.R.); sriosr@ull.edu.es (S.R.); sarmasri@ull.edu.es (S.d.A.-R.); lmartin@ull.edu.es (L.L.M.); imartin@ull.edu.es (I.R.M.)
3 Instituto de Estudios Avanzados en Atómica, Molecular y Fotónica (IUDEA), Universidad de La Laguna, E-38200 San Cristóbal de La Laguna, Spain
4 Institute of Photonic Technologies (LPT), Friedrich-Alexander-Universität Erlangen-Nürnberg (FAU), Konrad-Zuse-Straße 3/5, 91052 Erlangen, Germany; martin.hohmann@fau.de
5 Erlangen Graduate School in Advanced Optical Technologies (SAOT), Friedrich-Alexander-Universität Erlangen-Nürnberg (FAU), Paul-Gordan-Straße 6, 91052 Erlangen, Germany
6 Instituto de Materiales y Nanotecnología (IMN), Universidad de La Laguna, E-38200 San Cristóbal de La Laguna, Spain
* Correspondence: ksolerca@ull.edu.es (K.S.-C.); flahoz@ull.edu.es (F.L.)

**Abstract:** A novel application of microresonators for refractometric sensing in aqueous media is presented. To carry out this approach, microspheres of different materials and sizes were fabricated and doped with $Nd^{3+}$ ions. Under 532 nm excitation, the microspheres presented typical NIR $Nd^{3+}$ emission bands with superimposed sharp peaks, related to the Whispering Gallery Modes (WGMs), due to the geometry of the microspheres. When the microspheres were submerged in water with increasing concentrations of glycerol, spectral shifts for the WGMs were observed as a function of the glycerol concentration. These spectral shifts were studied and calibrated for three different microspheres and validated with the theoretical shifts, obtained by solving the Helmholtz equations for the electromagnetic field, considering the geometry of the system, and also by calculating the extinction cross-section. WGM shifts strongly depend on the diameter of the microspheres and their refractive index (RI) difference compared with the external medium, and are greater for decreasing values of the diameter and lower values of RI difference. Experimental sensitivities ranging from 2.18 to 113.36 nm/RIU (refractive index unit) were obtained for different microspheres. Furthermore, reproducibility measurements were carried out, leading to a repeatability of 2.3 pm and a limit of detection of $5 \times 10^{-4}$ RIU. The proposed sensors, taking advantage of confocal microscopy for excitation and detection, offer a robust, reliable, and contactless alternative for environmental water analysis.

**Keywords:** lanthanides; optofluidics; optical resonators; WGM; refractive index sensor; microspheres

Received: 18 December 2024
Revised: 14 January 2025
Accepted: 22 January 2025
Published: 24 January 2025

**Citation:** Soler-Carracedo, K.; Ruiz, A.; Ríos, S.; De Armas-Rillo, S.; Martín, L.L.; Hohmann, M.; Martín, I.R.; Lahoz, F. Stretching the Limits of Refractometric Sensing in Water Using Whispering-Gallery-Mode Resonators. *Chemosensors* **2025**, *13*, 33. https://doi.org/10.3390/chemosensors13020033



## 1. Introduction

At the present time, the control and management of water is attracting more and more awareness due to the increase in the population as well as of highly populated cities and, particularly, due to effects linked to global warming. Among the many elements that

are included in the control and management of water [1–3], one key element is the precise determination of any contaminants or pollutants that may affect the quality of the water supply. Nowadays, the most common devices used for water analysis rely on chemical analytical measurements, which require sampling and relatively costly and time-consuming analytical tests.

However, a promising strategy that is drawing increasing attention for the detection of contaminants in water is the use of optofluidic microsystems, particularly Whispering Gallery Mode (WGM) resonators. Unlike traditional methods requiring chemical analysis, WGM sensors provide semi-invasive, contactless detection and eliminate the need for chemical reagents. In addition, if they are integrated into the water flow, they can provide real-time detection of changes in the water composition, enhancing their utility for environmental surveillance and rapid response. WGM resonators are devices capable of trapping light through total internal reflection. They can be found in various forms and geometries such as microspheres, microdisks, microtoroids, optical rings, thin capillaries, etc. [4]. They can be used for a wide range of applications, including lasers [5–8], sensors [9–12], filters [13,14], communications [15], etc. Moreover, dye-doped WGM microlasers have proven their ability for protein detection in biological systems [7,8]. In the case of refractometric sensing, light is typically confined in close proximity to the surface of the WGM resonators. This leads to part of the light leaking outside the surface of the resonator, into the surrounding environment, in the form of evanescent waves, which explains the sensitivity of WGM to RI changes in the surrounding medium. Different optical sensors have been reported in the literature, based on a variety of optical structures and providing a wide range of sensor performances. For example, passive resonators based on silica or on $MgF_2$ microspheres have shown a limit of detection (LOD) of about $10^{-7}$ refractive index units (RIU) [16,17]. Silica thin capillary ring resonators have reported LODs as different as $3 \times 10^{-7}$ RIU or $10^{-3}$–$10^{-4}$ RIU [18,19]. Recently, silica-taped fibers coupled to cylindrical fibers have revealed LOD parameters of around $3 \times 10^{-5}$ RIU or $10^{-3}$ RIU [20,21]. Nevertheless, all these examples are passive resonators that share some common optical requirements. A high-resolution tunable IR laser or a broad band optical source is coupled to an optical fiber to be used as the probe light. In addition, although free space coupling to a microtoroid resonator has recently been reported [22], in most cases, the efficient excitation of the WGM requires a particular optical coupling of the evanescent wave of the probe light to the resonator, namely through the precise positioning of a tapered fiber in the near vicinity of the optical resonator [18–21], exact fabrication of fiber prism surfaces [16], or accurate and stable positioning of a coupling prism and the optical resonator [17]. These strict requirements can only be fulfilled in modern, well-equipped optical laboratories, requiring a great deal of expertise to maintain the experiments. Additionally, tapered fibers, i.e., the coupling system most frequently used [18–21], have a diameter of a few micrometers and tend to be fragile. However, for practical water environmental monitoring, a more robust, reliable sensor would be desirable.

In this work, we present an alternative approach to conventional WGM-based refractometric sensors. It is based on the free-space fluorescence emission of WGM from lanthanide-doped microsphere glasses. To accomplish this, we fabricate $Nd^{3+}$-doped optically active microspheres in a low-cost and straightforward manner. These microspheres are utilized in semi-invasive, contactless detection using commercial confocal microscopy, thus eliminating the need for fragile and complex optical coupling systems. Moreover, based on our fabrication capability, various microspheres with different sizes and made from different materials were fabricated and calibrated as sensors for RI changes in aqueous media, to determine the optimal sensor performance. This allows for a comprehensive study of the influence of two significant parameters, the size and the RI of the microspheres, on the sensor performance. We obtained a sensitivity of 113 nm/RIU, a

repeatability of 2.3 pm, and a minimum LOD of $5 \times 10^{-4}$ RIU. These results, together with the simplicity and robustness of the setup, show that this novel approach for refractometric sensing can be appealing as an optical sensor for practical water environmental surveillance.

## 2. Materials and Methods

### *2.1. Materials and Fabrication*

$Nd_2O_3$-SrO-BaO-$Nb_2O_5$-$B_2O_3$ (SBN:$Nd^{3+}$) glass was prepared via the melt-quenching method. To do so, commercial powders (Sigma-Aldrich, San Cristóbal de La Laguna, Spain) were mixed and melted in a platinum crucible for 1 h at 1400 °C in a furnace. The melt was then poured between two iron plates, resulting in a sample of 0.7 mm thickness. This sample was used to fabricate the first batch of microspheres [23]. To produce the microsphere, the SBN glass was first crushed into a fine powder. The resulting powder was then fed through a vertical furnace, where it underwent a melting process that created microspheres from the melted fine powder due to surface tension during the cooling process [24]. Microspheres fabricated by this method range from ~1 to over 100 μm in diameter. For the next batches of blend microspheres, the described method was used but with a powder made from a combination of SBN with either Schott glass or quartz, with a relationship of 5% to 95% in weight, respectively (see Figure 1a).

Dilutions of glycerol ($n_{532nm}$ = 1.4739) in water ($n_{532nm}$ = 1.33303) were prepared to be used as the standard for RI sensor calibration; the concentration of glycerol in water ranged from 0 to 39.5%, corresponding to RI from 1.3352 to 1.3900 [25]. These RI values were verified using an Abbe refractometer.

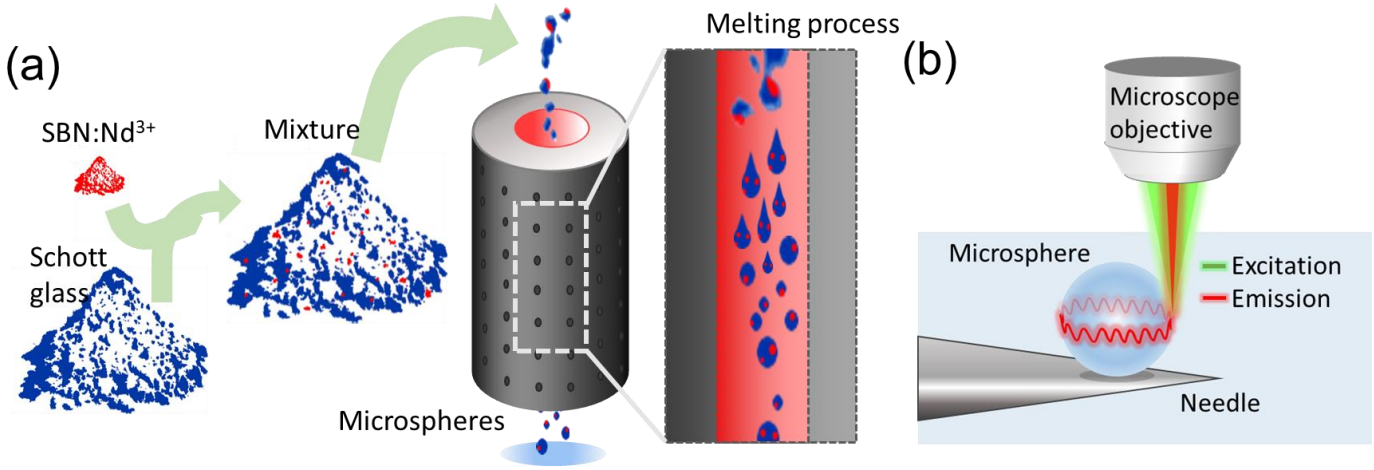


**Figure 1.** Scheme of (**a**) the fabrication process used to obtain $Nd^{3+}$-doped microspheres and (**b**) WGM detection using a confocal microscope.

### *2.2. Optical Characterization*

Emission spectra were recorded using a Renishaw InVia confocal micro-Raman system in a front-face detection geometry configuration, focused with a ×20 Olympus SLMPlan long-working-distance microscope objective. The Renishaw InVia system was set up with a grating of 1800 grooves/mm and a power-controlled 100 mW 532 nm laser diode at 5% laser power (2 μW/μm² power density).

To measure the WGM shifts as a function of the RI of a medium, the microspheres were attached to the tip of a needle using hot-melting adhesive. Later, the needle was submerged and fixed in a small container filled with deionized water on top of a concave microscope slide (see Figure 1b). Spectral shifts were achieved by using the different dilutions described in the previous section. To assure the stability of the measurements, a

low power excitation laser was used to avoid heating and, additionally, at least 3 min of waiting time between measurements was considered to ensure thermal equilibrium. Measurements were conducted in a controlled temperature room.

The spectral resolution provided by the manufacturer of the equipment was 30 pm. However, we estimated the actual spectral resolution of our experimental setup with the commonly used 3σ rule, where σ stands for the mean standard deviation of the Gaussian fitting of a narrow bandwidth emission measurement (see Results and Discussion section). A more conservative spectral resolution of $\Delta\lambda_{min}$ = 60 pm was obtained, meaning the smallest change in wavelength that can be detected. Additionally, the repeatability of the measurements was determined. For that purpose, a set of 100 measurements were conducted under exactly the same conditions. All the measurements were conducted in water without glycerol at ambient conditions. From the spectra obtained, the position of the modes was calculated by fitting the experimental bands to a Gaussian curve. Afterwards, a statistical analysis from the resulting positions was carried out to obtain the standard deviation, and the repeatability was set as three times this value. The described method takes into account not only the reliability of the microresonator, but also that of the experimental setup, including laser fluctuations, temperature fluctuation at the laboratory, electric noise, etc.

## 3. Results and Discussion

### *3.1. $Nd^{3+}$-Doped SBN Microspheres*

Figure 2a shows the characteristic emission spectrum, in the NIR range, from a bulk glass sample of SBN:$Nd^{3+}$ under 532 nm excitation. In this spectrum, two broad bands centered at 900 and 1060 nm can be seen, related to the $^4F_{3/2} \rightarrow {}^4I_{9/2}$ and $^4F_{3/2} \rightarrow {}^4I_{11/2}$ $Nd^{3+}$ transitions, respectively. When the emission spectrum is obtained from a microsphere fabricated from the same glass, and the confocal microscope is focused at the edge of the microsphere, a drastic change can be observed in the spectrum, as a series of narrow peaks appear, superimposed to the $Nd^{3+}$ emission bands (see Figure 2b). These peaks are related to the WGM phenomenon. We wish to remark that focusing the confocal microscope at the edge of the microsphere was a key factor in enhancing the detection of the WGM. Moreover, two families of about evenly spaced WGM peaks are clearly observable in Figure 2b. One set of peaks is more intense (about two or three times higher) than the other one. The most intense family peaks correspond to the TE modes, which are preferentially detected because of the higher efficiency of the diffraction grating of the spectrometer. Therefore, the rest of the WGM spectral shift analysis was conducted for the TE modes to improve the signal-to-noise ratio.

The quality factor, $Q$ factor, of the microresonator is given by

$$Q = \frac{\lambda_m}{\Delta\lambda_m} \quad (1)$$

where $\lambda_m$ represents the wavelength of the WGM and $\Delta\lambda_m$ is the linewidth of the WGM. The spectral position and linewidth of the WGM observed in Figure 2b were obtained by fitting the peaks to Lorentzian or to Gaussian curves. Due to the limited spectral resolution of the spectrometer, it was not possible to distinguish the Lorentzian from the Gaussian fit. Therefore, Gaussian fittings have been used in the rest of the paper. A $Q$ factor of about $1.7 \times 10^4$ was obtained.

As a first approximation, the spectral position of the WGM can be calculated using the geometrical optics approach given by

$$m\lambda_m = 2 \cdot \pi \cdot n \cdot R \quad (2)$$

where $m$ represents the mode number, $\lambda_m$ is the wavelength at which the WGM occurs, $R$ is the radius of the microsphere, and $n$ is its refractive index.

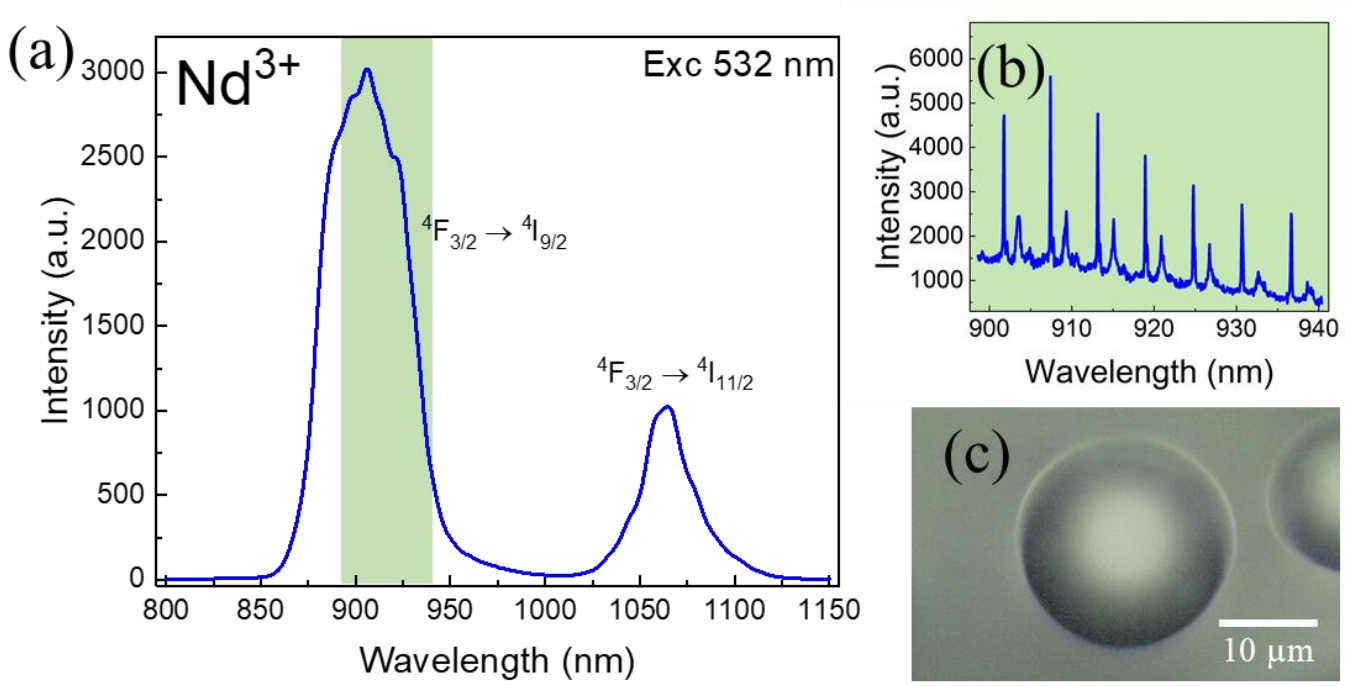


**Figure 2.** (**a**) Bulk sample NIR emission spectrum of SBN:$Nd^{3+}$, (**b**) emission spectrum from the highlighted zone obtained from a ~23 µm diameter microsphere fabricated from the same bulk material, and (**c**) optical image of the microsphere.

The spectral distance between two adjacent WGMs is known as the free spectral range (FSR), and is given by

$$FSR = \frac{\lambda^2}{2 \cdot \pi \cdot n \cdot R} \quad (3)$$

The averaged FSR value observed for the peaks shown in Figure 2b is about 5.72 nm. The radius R of the microsphere under excitation has been estimated from an optical image of the sample, see Figure 2c, yielding a value of about ~12.5 µm. Taking into account Equation (3), this leads to $n$ = 2.00, which agrees with the RI value reported for the bulk glass [26].

To measure the WGM as a function of changes in the RI of a medium, a microsphere of diameter 23 µm was glued to the tip of a needle and submerged in a container filled with deionized water (see Materials and Methods). The change in RI was achieved by increasing the concentration of glycerol in the water. All the WGMs started to shift towards higher wavelengths as the RI of the solution increased, as shown in Figure 3a. The mean shifts in four WGMs, located in the range from 900 to 920 nm, were recorded from normal water ($n$~1.333) to water with a concentration of 34.42% glycerol ($n$~1.385). A total mean shift of 0.335 nm was obtained, see Figure 2b, indicating a sensitivity, S, of 6.39 nm/RIU.

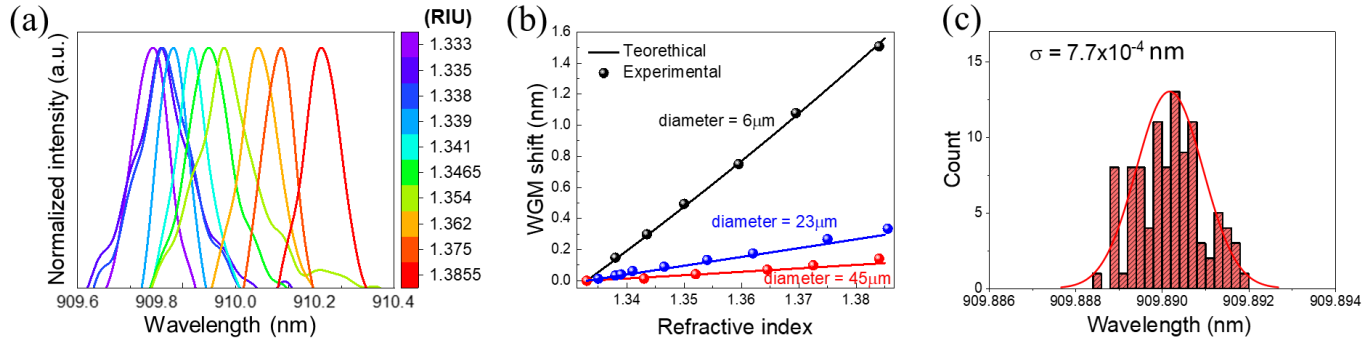


**Figure 3.** (**a**) Fittings of a single WGM peak when changing the RI in the outside medium. (**b**) Experimentally (scatter) and theoretically (line) determined WGM shift as a function of the RI of the outside medium, for SBN:$Nd^{3+}$ microspheres of RI 2 and with diameters 6, 23, and 45 μm (black, blue, and red, respectively). (**c**) Histogram of the distribution of WGM uncertainty.

The theoretical analysis of WGM has been performed assuming a homogeneous dielectric optical microsphere with refractive index $n$, surrounded by a uniform external medium with refractive index $n_0$. In this model, the analytical solutions of the WGM can be obtained from the solution of the Helmholtz equation for the electromagnetic field in spherical coordinates, together with appropriate boundary conditions at the interface between the dielectric sphere and the external medium. In particular, the resonances are obtained from the characteristic equation resulting from matching the tangential electric and magnetic fields across the surface of the sphere. This leads to the following dispersion relation [27]:

$$P\frac{\psi_l'(kR)}{\psi_l(kR)} = \frac{\xi_l'(k_0R)}{\xi_l(k_0R)} \tag{4}$$

with $P = n/n_0$ for the TE modes and $P = n_0/n$ for the TM modes, $k = 2\pi n/\lambda$ and $k_0 = 2\pi n_0/\lambda$ for the wavenumbers, and the functions

$$\psi_l(x) = \sqrt{\frac{\pi x}{2}} J_{l+1/2}(x) \tag{5}$$

and

$$\xi_l(x) = \sqrt{\frac{\pi x}{2}} H^{(2)}_{l+1/2}(x) \tag{6}$$

where $J_{l+1/2}(x)$ is the Bessel function of the first kind and $H^{(2)}_{l+1/2}(x)$ the Hankel function of the second kind. For a given value of the mode number $l$, the wavelengths $\lambda$ for which resonances occur are obtained by numerically solving the dispersion relation. The displacement of the WGM peaks as the refractive index $n_0$ of the external medium changes is then analyzed.

As can be seen in Figure 3b, by setting the RI of the microsphere to $n = 2$ and the diameter to 23 μm, and changing the RI of the outside medium, a good agreement between the experimental WGM shifts and the theoretically calculated TE WGM shifts was observed.

The resonance shifts were also estimated by calculating the extinction cross-section given by the expression

$$C_{ext} = \frac{2 \cdot \pi}{k^2} \sum_{i=1}^{\infty} (2i+1)\, Re(a_i + b_i) \tag{7}$$

where $a_i$ and $b_i$ are the scattering coefficients and k the wave number [27]. The WGM manifest as a ripple structure superimposed onto the extinction cross-section, and occurred when the denominators of $a_i$ and $b_i$ were minima [28,29]. The results obtained for the WGM shifts agree with those obtained with the Helmholtz equation.

It is also known that the WGM shift as a function of the outside RI depends on the diameter of the microsphere [17]. The amount of energy of the WGM associated with the evanescent wave increases as the curvature of the microspheres becomes higher, that is, when the diameter of the microspheres decreases. As the evanescent field travels in the outside medium, it is sensitive to changes in $n$. Consequently, an enhancement in S is expected as the diameter of the microspheres decreases. In order to verify this dependence, the previous experiment was repeated, but this time for microspheres of larger and smaller diameter (6 and 45 μm, respectively). With the new microspheres, a similar redshift was observed, but this time total shifts of 0.75 and 0.14 nm were obtained for the microspheres with 6 and 45 μm in diameter, respectively, and with S values of 29.93 and 2.18 nm/RIU. These results show that sensitivity strongly depends on the diameter of the spheres, showing a supra-linear dependence. Indeed, the sensitivity increased significantly as the diameter of the microsphere decreased. In particular, the 6 μm diameter microsphere presented a sensitivity more than one order of magnitude higher than that of the microsphere with a diameter of 45 μm. This is a significant observation, since slight improvements in the fabrication and selection of microspheres could lead to substantial increments in the sensitivity of the sensor.

Lastly, the repeatability in the determination of the spectral position of the WGM was obtained using a 23 μm-diameter microsphere and conducting 100 measurements of the WGM emission spectrum (see Materials and Methods). The value of the repeatability obtained by this method was established at 2.3 pm, as can be seen in Figure 3c.

### *3.2. $Nd^{3+}$-Doped Blend Microspheres*

In order to enhance the evanescent wave associated with the WGM, microspheres from different materials with lower RI were fabricated. It is known that both the diameter and the RI of the material of the resonator can lead to an increase in the evanescent wave of the WGM and, consequently, enhance the sensitivity to changes in the RI of the environment of the microspheres. In particular, the surrounding medium of the microspheres is basically water ($n$ = 1.333) with different glycerol contents. If the $n$ contrast between the microspheres and the outside medium decreases, the fraction of the evanescent wave of the WGM increases and, consequently, higher S is expected. A way to reduce the $n$ contrast is to mix the SBN:$Nd^{3+}$ starting material with others with lower $n$ values.

The new microspheres were fabricated from a mixture of quartz ($n$~1.45) with SBN:$Nd^{3+}$ ($n$~2.00) or from a blend of Schott glass ($n$~1.51) and SBN:$Nd^{3+}$ ($n$~2.00). In both cases, there was a 95 to 5% concentration in weight, and the SBN:$Nd^{3+}$ component acted as the luminescent element of the mixture (see Materials and Methods). The new microspheres, selected to have a similar diameter (around 25–30 μm), were submerged in water with increasing concentrations of glycerol, as in the previous experiment. The resulting mean WGM shifts as a function of the $n_0$ value of the surrounding medium are presented in Figure 4. An increase in the WGM shifts as the RI of the microspheres decreases can clearly be seen, with S values of 113.36, 23.02, and 5.67 nm/RIU for the quartz–SBN blend, Schott glass–SBN blend, and pure SBN microspheres, respectively. In terms of relative sensitivity, $S_R$ [30], this corresponds to values of around 13.44, 3.38, and 0.63%/RIU, respectively.

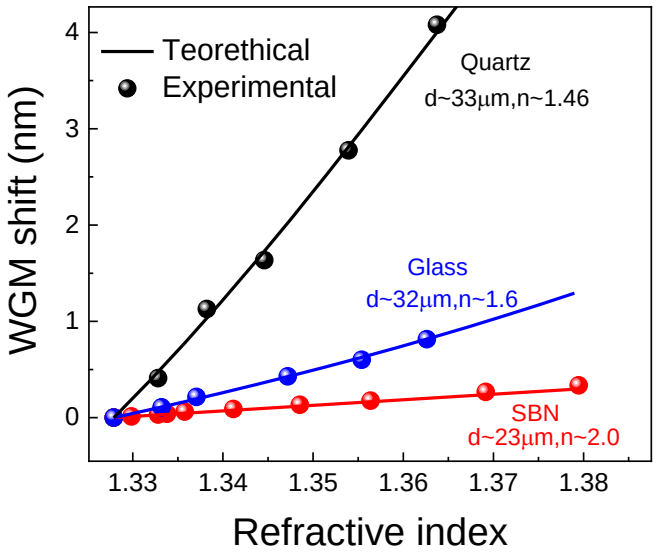


**Figure 4.** Experimentally (scatter) and theoretically (line) determined WGM shift for microspheres with different diameters and inner RI (black: d~33 μm, *n*~1.46; blue: d~32 μm, *n*~1.6; red: d~23 μm, *n*~2) as a function of changes in the outside medium RI.

From the results presented in Figure 4, it can be clearly seen that, by decreasing the inner RI of the resonator, S increases in a supralinear way as the RI approaches that of the outside medium. Indeed, we have both experimentally observed and theoretically calculated an actual improvement of around two orders of magnitude in the set of microspheres studied in this investigation. For comparison purposes, a large variety of S values are reported in the literature. S parameters of 30 nm/RIU and 30 nm/RIU can be observed in silica and $MgF_2$ microspheres [16,17]; values of 570 nm/RIU and 390 nm/RIU have been published for silica thin capillaries ring resonators [18,19]; and S = 100 nm/RIU or 83 nm/RIU are found in silica-taped fibers coupled to cylindrical fibers [20,21].

Nevertheless, perhaps the most interesting parameter to evaluate the performance of a sensor is its LOD, which is defined as the smallest change in the RI that can be detected. It is proportional to the spectral resolution, $\Delta\lambda_{min}$, and inversely proportional to the sensitivity, S, of the sensor:

$$LOD = \frac{\Delta\lambda_{min}}{S} \quad (8)$$

The lowest LOD parameter in this study was obtained for the optical microresonator with the highest S, that is, the $Nd^{3+}$-doped quartz–SBN alloy, with a 33 μm diameter and a value of LOD = $5 \times 10^{-4}$ RIU. As was indicated in the Introduction section, a wide variety of LOD parameters ranging from $10^{-3}$ RIU to $10^{-7}$ RIU have been reported depending on the fabrication process and optical resonator geometry [16–21]. As an application example, the fluorescent WGM optical sensor described in this paper could be used in water quality surveillance in populated or industrial environments. Indeed, one of the most frequently found water pollutants in household greywater (domestic wastewater from households or office buildings that does not include human waste) are detergents [31]. Moreover, in an effort towards more sustainable water management habits, greywater reuse for gardening has been proposed [32,33]. However, it has been observed that the content of surfactants in greywater may damage the growth of some crops. On the other hand, if the used greywater had a low detergent content, the plants grew without any damage, provided it was below the established harmful level of 5 mg/mL [34–36]. According to our recent investigations [31], the LOD found for our luminescent $Nd^{3+}$-doped-

blend microsphere glasses would allow a detection of detergent concentration in water of 5 mg/mL, showing their usefulness for water environmental analyses.

## 4. Conclusions

In conclusion, optically active microspheres were fabricated from bulk samples of SBN:$Nd^{3+}$ glass and also by blends of quartz—SBN:$Nd^{3+}$ and Schott glass—SBN:$Nd^{3+}$, which allowed a reduction in the RI of the resulting material. Microspheres ranging from ~1 to over 100 μm in diameter were produced by this method. Under 532 nm excitation, the obtained microspheres presented the typical NIR $Nd^{3+}$ emission with superimposed WGM related to the geometry of the microspheres. When the microspheres were submerged in water mixed with different concentrations of glycerol, spectral shifts for the WGM were observed. These shifts were studied for different diameters, as well as different microsphere RI. The experimental results obtained were in good agreement with the theoretical calculations in all cases. Spectral shifts ranging from 2.18 to 113.36 nm/RIU were obtained for the microspheres with highest and lowest diameter and RI, respectively. Furthermore, reproducibility measurements were carried out, leading to a repeatability limit of 2.3 pm, and the limit of detection of the optical sensor was estimated to be about $5 \times 10^{-4}$ RIU.

It is important to mention that, by changing the lanthanide ion used as a dopant element, it is possible to tune both the absorption and emission spectrum of the final sensor. This novel approach to water environment refractometric sensing, based on the fluorescence evanescent wave coupling of WGM from luminescent rare-earth-doped microspheres, showcases several practical advantages as compared to other WGM resonators that require precise optical alignment between fragile tapered fibers or prisms customized to the resonator. Our method allows semi-invasive analysis (remote observation), robust reproducibility, and high spectral resolution without the need for external coupling or stringent alignment, relying instead on commercially available confocal microscopy. The simplicity and affordability of this fabrication method positions these sensors as practical tools for environmental water monitoring, with potential applications in real-time pollutant detection.

**Author Contributions:** Conceptualization, K.S.-C. and F.L.; methodology, S.d.A.-R., K.S.-C. and F.L.; validation, I.R.M., M.H. and F.L.; formal analysis, K.S.-C., S.R., and A.R.; investigation, S.d.A.-R., L.L.M., and K.S.-C.; resources, F.L., I.R.M. and A.R.; data curation, S.d.A.-R. and K.S.-C.; writing—original draft preparation, K.S.-C. and F.L.; writing—review and editing, K.S.-C., S.d.A.-R., A.R., S.R., L.L.M., M.H., I.R.M. and F.L.; visualization, K.S.-C. and S.d.A.-R.; supervision, F.L. and I.R.M.; project administration, K.S.-C. and F.L.; funding acquisition, A.R. and F.L. All authors have read and agreed to the published version of the manuscript.

**Funding:** We acknowledge financial support from the National Science Centre Poland, Opus Grant No. 2022/45/B/ST5/00604, Ministerio de Ciencia e Innovación/Agencia Estatal de Investigación from the Spanish Government, and "ERDF (FEDER) A way of making Europe", under projects PID2019-107335RA-I00, PID2022-136566NB-I00, and PID2022-138269NB-I00.

**Institutional Review Board Statement:** Not applicable.

**Informed Consent Statement:** Not applicable.

**Data Availability Statement:** The data that support the findings of this study are available at the following link (1 January 2025): https://doi.org/10.5281/zenodo.12583754.

**Conflicts of Interest:** The authors declare no conflicts of interest. The funders had no role in the design of the study; in the collection, analyses, or interpretation of data; in the writing of the manuscript; or in the decision to publish the results.

## References


1. Velasco-Muñoz, J.F.; Aznar-Sánchez, J.A.; Belmonte-Ureña, L.J.; Román-Sánchez, I.M. Sustainable Water Use in Agriculture: A Review of Worldwide Research. *Sustainability* **2018**, *10*, 1084.
2. Oral, H.V.; Carvalho, P.; Gajewska, M.; Ursino, N.; Masi, F.; van Hullebusch, E.D.; Kazak, J.K.; Exposito, A.; Cipolletta, G.; Andersen, T.R.; et al. A review of nature-based solutions for urban water management in European circular cities: A critical assessment based on case studies and literature. *Blue-Green Syst.* **2020**, *2*, 112–136.
3. Berglund, E.Z.; Pesantez, J.E.; Rasekh, A.; Shafiee, M.E.; Sela, L.; Haxton, T. Review of Modeling Methodologies for Managing Water Distribution Security. *J. Water Resour. Plan. Manag.* **2020**, *146*, 1–23.
4. Saleh, B.E.A.; Teich, M.C. *Fundamentals of Photonics*; John Wiley & Sons: Hoboken, NJ, USA, 2019.
5. Yang, S.; Wang, Y.; Sun, H. Advances and Prospects for Whispering Gallery Mode Microcavities. *Adv. Opt. Mater.* **2015**, *3*, 1136–1162.
6. Wen, K.; Cao, Y.; Gu, L.; Wang, S.; Qian, D.; Wang, J.; Kuang, Z.; Luo, M.; Wang, G.; Guan, S.; et al. Continuous-Wave Lasing in Perovskite LEDs with an Integrated Distributed Feedback Resonator. *Adv. Mater.* **2023**, *35*, e2303144.
7. Wang, Z.; Fang, G.; Gao, Z.; Liao, Y.; Gong, C.; Kim, M.; Chang, G.-E.; Feng, S.; Xu, T.; Liu, T.; et al. Autonomous Microlasers for Profiling Extracellular Vesicles from Cancer Spheroids. *Nano Lett.* **2023**, *23*, 2502–2510.
8. Mao, W.; Gao, X.; Li, B.; Zhang, Y.; Wang, P.; Dong, H.; Zhang, L. Randomized whispering-gallery-mode microdisk laser arrays via cavity deformations for anti-counterfeiting labels. *Photonics Res.* **2023**, *11*, 1227.
9. Jiang, X.; Qavi, A.J.; Huang, S.H.; Yang, L. Whispering Gallery Microsensors: A review. *Matter* **2020**, *3*, 371–92.
10. Yu, D.; Humar, M.; Meserve, K.; Bailey, R.C.; Nic Chormaic, S.; Vollmer, F. Whispering-gallery-mode sensors for biological and physical sensing. *Nat. Rev. Methods Prim.* **2021**, *1*, 83.
11. Zhang, C.; Pu, S.; Liu, W.; Hao, Z.; Xu, T.; Duan, S.; Fu, J.; Han, S. Simultaneous measurement of bidirectional magnetic field and temperature with a dual-channel sensor based on the whispering gallery mode. *Opt. Express* **2024**, *32*, 19541.
12. Zhang, C.; Pu, S.; Hao, Z.; Wang, B.; Yuan, M.; Zhang, Y. Magnetic Field Sensing Based on Whispering Gallery Mode with Nanostructured Magnetic Fluid-Infiltrated Photonic Crystal Fiber. *Nanomaterials* **2022**, *12*, 862.
13. Yu, W.; Xu, L.; Zhang, X.Y.; Chen, J.-X. Dual-Band Dual-Mode Dielectric Resonator Filtering Power Divider With Flexible Output Phase Difference and Power Split Ratio. *IEEE Trans. Microw. Theory Tech.* **2022**, *70*, 190–199.
14. Jin, L.; Di Lauro, L.; Pasquazi, A.; Peccianti, M.; Moss, D.J.; Morandotti, R.; Little, B.E.; Chu, S.T. Optical multi-stability in a nonlinear high-order microring resonator filter. *APL Photonics* **2020**, *5*, 056106.
15. Gizatulin, A.; Sultanov, A. Application of whispering gallery modes (WGM) in optical communications. In *Optical Technologies in Telecommunications 2017*; Andreev, V.A., Burdin, V.A., Morozov, O.G., Sultanov, A.H., Bourdine, A.V., Eds.; SPIE: Bellinghan, WA, USA, 2018; p. 22.
16. Hanumegowda, N.M.; Stica, C.J.; Patel, B.C.; White, I.; Fan, X. Refractometric sensors based on microsphere resonators. *Appl. Phys. Lett.* **2005**, *87*, 201107.
17. Sedlmeir, F.; Zeltner, R.; Leuchs, G.; Schwefel, H.G. High-Q MgF_2 whispering gallery mode resonators for refractometric sensing in aqueous environment. *Opt. Express* **2014**, *22*, 30934.
18. Li, H.; Fan, X. Characterization of sensing capability of optofluidic ring resonator biosensors. *Appl. Phys. Lett.* **2010**, *97*, 011105.
19. Zamora, V.; Díez, A.; Andrés, M.V.; Gimeno, B. Refractometric sensor based on whispering-gallery modes of thin capillarie. *Opt. Express* **2007**, *15*, 12011.
20. Eryürek, M.; Karadag, Y.; Ghafoor, M.; Bavili, N.; Cicek, K.; Kiraz, A. Liquid refractometric sensors based on optical fiber resonators. *Sens. Actuators A Phys.* **2017**, *265*, 161–167.
21. Hassan, E.A.; Al-Mfrji, A.A.; Mahmood, A.I. Wavelength Tuning of the Cylindrical Structure Whispering Gallery Mode Micro-Resonator for Sensing Applications. *J. Opt.* **2024**, 1–9. https://doi.org/10.1007/s12596-024-01964-1.
22. Suebka, S.; McLeod, E.; Su, J. Ultra-high-Q free-space coupling to microtoroid resonators. *Light. Sci. Appl.* **2024**, *13*, 75.
23. Haro-González, P.; Martín, I.R.; Arbelo-Jorge, E.; González-Pérez, S.; Cáceres, J.M.; Núñez, P. Laser irradiation in Nd3+ doped strontium barium niobate glass. *J. Appl. Phys.* **2008**, *104*, 013112.
24. Elliott, G.R.; Hewak, D.W.; Murugan, G.S.; Wilkinson, J.S. Chalcogenide glass microspheres; their production, characterization and potential. *Opt. Express* **2007**, *15*, 17542.
25. Aldoğan, K.Y.; İde, C. Experimental Investigation of Refractive Index Measurement of Common Solvents and Aqueous Solutions in the Infrared Wavelengths. *Balk. J. Electr. Comput. Eng.* **2018**, *6*, 159–164.
26. Ewbank, M.D.; Neurgaonkar, R.R.; Cory, W.K.; Feinberg, J. Photorefractive properties of strontium-barium niobate. *J. Appl. Phys.* **1987**, *62*, 374–380.

27. Bohren, C.F.; Huffman, D.R. *Absorption and Scattering of Light by Small Particles*; John Wiley & Sons: Hoboken, NJ, USA, 2008.
28. Mishchenko, M.I.; Videen, G.; Yang, P. Extinction by a homogeneous spherical particle in an absorbing medium. *Opt. Lett.* **2017**, *42*, 4873–4876.
29. Chýlek, P.; Zhan, J. Interference structure of the Mie extinction cross section. *J. Opt. Soc. Am. A* **1989**, *6*, 1846–1851.
30. Wade, S.A.; Collins, S.F.; Baxter, G.W. Fluorescence intensity ratio technique for optical fiber point temperature sensing. *J. Appl. Phys.* **2003**, *94*, 4743–4756.
31. Lahoz, F.; de Armas-Rillo, S.; Hernández-Rodríguez, C.; Gil-Rostra, J.; Yubero, F. Optical monitoring of detergent pollutants in greywater. *Opt. Express* **2023**, *31*, 15227.
32. Al-Jayyousi, O.R. Greywater reuse: Towards sustainable water management. *Desalination* **2003**, *156*, 181–192.
33. Finley, S.; Barrington, S.; Lyew, D. Reuse of Domestic Greywater for the Irrigation of Food Crops. *Water Air Soil Pollut.* **2008**, *199*, 235–245.
34. Misra, R.K.; Patel, J.H.; Baxi, V.R. Reuse potential of laundry greywater for irrigation based on growth, water and nutrient use of tomato. *J. Hydrol*. **2010**, *386*, 95–102.
35. Lado, M.; Ben-Hur, M. Treated domestic sewage irrigation effects on soil hydraulic properties in arid and semiarid zones: A review. *Soil Tillage Res.* **2009**, *106*, 152–163.
36. Sawadogo, B.; Sou, M.; Hijikata, N. Effect of Detergents from Greywater on Irrigated Plants: Case of Okra (*Abelmoschus esculentus*) and Lettuce (*Lactuca sativa*) (Desert Technology 11 International Conference). *J. Arid. Land Stud.* **2014**, *24*, 117–120.